Electron degradation and yields of initial products. IX. Subexcitation electrons in a mixture of molecular oxygen and molecular nitrogen

M. A. Ishii,* Mineo Kimura,† and Mitio Inokuti
Argonne National Laboratory, Argonne, Illinois 60439
(Received 10 April 1991; revised manuscript received 12 August 1991)

The behavior of subexcitation electrons in gaseous mixtures of O_2 and N_2 is studied by using the Spencer-Fano theory and its simplified continuous-slowing-down approximation. Because of its strong resonance around 2 eV, N_2 is overwhelmingly dominant over O_2 in energy-loss processes. Addition of N_2 to O_2, even a few percent, causes significant changes in some yields of O_2. In particular, yields for electron attachment and rotational excitation for O_2 show a strong nonlinearity as a function of composition, while all yields of N_2 depend linearly on composition.

PACS number(s): 33.80.Eh, 51.10.+y, 34.50.Bw, 34.80.Gs

I. INTRODUCTION

The behavior of subexcitation electrons in pure gases has been extensively studied, e.g., in molecular nitrogen [1], carbon monoxide [2], molecular oxygen [3], and water [4]. Major findings of these studies concern (i) the effect of resonances in a cross section on the degradation process, (ii) the role of electronic excitations having lower thresholds that overlap with those of vibrational and rotational excitations, (iii) the role of negative-ion formation processes that compete with the degradation, and (iv) the validity of the continuous-slowing-down approximation (CSDA) compared with the Spencer-Fano (SF) theory. In many respects, the understanding of these points constitutes a significant basis for radiation physics and chemistry.

A natural extension of these studies is the treatment of mixtures. The study of a mixture is important, particularly in the following respects: (i) a medium of interest in most applications, most notably in radiation chemistry and biology, is a complex of mixture of various molecules, and (ii) our theoretical tools, the SF and the CSDA, have not been exposed to systematic tests for mixtures. It is essential to investigate the similarities and the differences in the degradation spectra of a mixture and its component gases and to find the principles that govern the dependence upon the composition. Bearing this in mind, we chose the mixture of molecular oxygen and molecular nitrogen. This mixture is notable in two respects. First, the vibrational excitation cross sections in both O_2 and N_2 show strong resonances in different energy regions (around 1 eV for O_2 and around 2.5 eV for N_2), and the cross sections have magnitudes of 10^{-17} and 10^{-16} cm^2, respectively. Second, nitrogen and oxygen are the main constituents of the earth's atmosphere and the behavior of electrons is important to the understanding of the chemistry, especially that of the upper atmosphere. As in our previous series of papers [1–4], we treat the moderation of subexcitation electrons until their energies reach about 0.1 eV which is sufficiently above their thermal energy at room temperature. We assume that our treatment concerns the early stage of electron irradiation in the gaseous mixture and that secondary energy and particle transfers (chemical reactions) take place much later [5]. Calculations are carried out for the temperature of 0 °C and the pressure of 1 atm.

II. SUMMARY OF THEORY

A. Spencer-Fano equation and its extension to mixtures

A detailed account of the Spencer-Fano equation and its extension to mixtures has been given elsewhere [6]. Therefore only a brief review is presented here as a basis for later discussion. Electron degradation can best be discussed in terms of the electron degradation spectrum (or track length distribution), $y(T)$, which satisfies the SF equation

$$nK_T y(T)+u(T)=0 . \tag{1}$$

To be specific, $y(T)dT$ is the total track length of electrons having energies between T and $T+dT$, n is the number density of molecules, $u(T)dT$ represents the number of source electrons of energies between T and $T+dT$, and K_T represents a cross-section operator defined by

$$K_T(T)y(T)=\int dT' y(T')q(T';T)-y(T)\int dT'' q(T;T'') , \tag{2}$$

where $q(T';T)dT'$ is the cross section for a collision in which an electron's energy changes from $T'+dT'$ to T. Equation (2) represents the net gain or loss of electrons at T in a gas of unit density.

Let us consider a mixture with a total number density n, composed of $n^{(1)}$ particles per unit volume species 1, $n^{(2)}$ particles per unit volume of species 2, etc., such that

$$n=\sum_{\lambda} n^{(\lambda)} . \tag{3}$$

Then, we may write

$$nK_T = \sum_{\lambda} n^{(\lambda)} K_T^{(\lambda)} , \tag{4}$$

where $K_T^{(\lambda)}$ is the cross-section operator of the species λ as defined in Eq. (2). Then, Eq. (1) applies to mixtures as well.

Let us denote the solution of Eq. (1) with the unit monoenergetic source $u(T)=\delta(T-T_0)$ as $y(T_0,T)$. The yield $N_i^{(\lambda)}(T_0)$ of a process i by the molecules of species λ that is due to complete degradation initiated by an electron of energy T_0 and terminated by threshold energy T_f can be calculated as

$$N_i^{(\lambda)}(T_0) = n^{(\lambda)} \int_{T_f}^{T_0} dT\, y(T_0,T) \sigma_i^{(\lambda)}(T) , \tag{5}$$

where $\sigma_i^{(\lambda)}(T)$ is the cross section for process i of the species λ for an electron of energy T.

Extension of the CSDA to account for mixtures follows similarly. In general, the total stopping power becomes the weighted sum of the individual stopping powers attributed to the respective species in the mixture.

B. Cross sections

The cross sections used in our calculations were compiled by Itikawa *et al.* [7,8] for oxygen and nitrogen. Their effects on electron degradation for a single medium have already been discussed in some detail [1,3]. Therefore only key elements will be discussed here.

The primary moderating factor in electron degradation is the pronounced resonance effect associated with the temporary capture of an incident electron. This effect manifests itself most strongly in vibrational excitation cross sections in oxygen around 1 eV and nitrogen around 2.5 eV. As noted earlier, the separation of each molecule's resonance region was one of the prime reasons for the choice of these particular molecules to examine which resonance in electron degradation is dominantly governing the degradation and to what degree. It will be shown that the resonance effects in nitrogen, particularly those in vibrational (vib)(0→1), vib(0→2), and rotational (rot)(0→2) excitations, are the dominant factors in electron moderation over most of the degradation spectrum. That is, the "signature" that is characteristic of nitrogen in the degradation will be seen clearly even at very low concentrations of nitrogen in the mixture (see Sec. III A).

Oxygen cross sections are relatively smooth, particularly in the region where the nitrogen has a resonance at 2.5 eV. In the lower-energy region, where one finds the sharp resonance cross sections of oxygen-vib(0→1) excitations and no strong competitors for the moderation are present, we expect this process to have a strong influence on the degradation, even though a large amount of N_2 is introduced.

It is appropriate to state certain qualifications on the cross-section data for oxygen that were given by Itikawa *et al.* [8], which we have adopted for use in the present work. The data of Ref. [8] are primarily based on beam measurements. Another school of thought, represented by Gousset *et al.* [9], puts greater weight on electron-swarm measurements, and recommends an appreciably different set of cross-section values. For example, according to Ref. [9], an electronic excitation with an energy loss of 4.5 eV has a cross section at 6.0 eV amounting to about 60% of that for the vibrational-excitation cross section given in Ref. [8]. The inclusion of this electronic excitation would modify the electron-degradation kinetics and its consequences such as the yield of O^- ions. Another implication of the swarm data concerns lower energies: there are indications that the cross sections of Refs. [7] and [8] lead to an overestimation of the relative role of N_2 in the energy loss. Indeed, the swarm data seem to indicate [10] that the primary energy loss of electrons below 1 eV in dry air is due to O_2. Finally, according to Lawton and Phelps [11], the energy loss to vibrational excitation as given in Ref. [8] is too small, by about a factor of 2, to account for the transport coefficients measured in the swarm experiments. Because of these qualifications on the cross-section data, our present work remains somewhat provisional.

III. RESULTS

A. Degradation spectrum

Degradation spectra for pure oxygen [3] and pure nitrogen [1] have previously been reported along with extensive discussions. Hence, we will present these results in Figs. 1 and 2, respectively, for comparison without much detailed discussion. We should note, however, that the nitrogen spectrum is slightly different from that previously presented [1] because we included in the present calculation a second (0→2) vibrational excitation that was omitted from the previous work. The general shapes and structures are nearly the same as before, but we notice that the region between 3.8 and 1.5 eV shows additional higher-frequency oscillations superimposed on the simpler spectrum shown before [1]. This alteration is a direct consequence of introducing the (0→2) vibrational excitation to the calculation and is explained by the fact that the (0→2) vibrational-excitation cross section is slightly out of phase with the (0→1) vibrational-excitation cross section. Naturally, we expect yields for N_2 to be slightly redistributed because of the additional

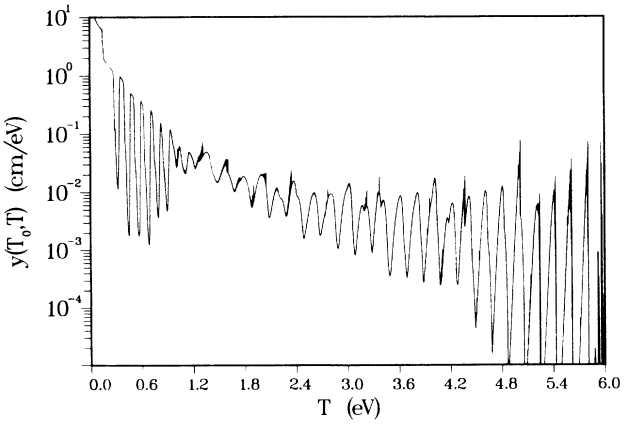

FIG. 1. Electron-degradation spectrum of a 6-eV electron in 100% O_2.

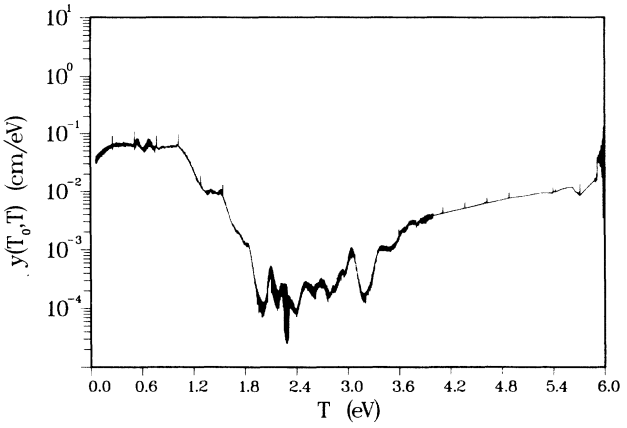

FIG. 2. Electron-degradation spectrum of a 6-eV electron in 100% N_2.

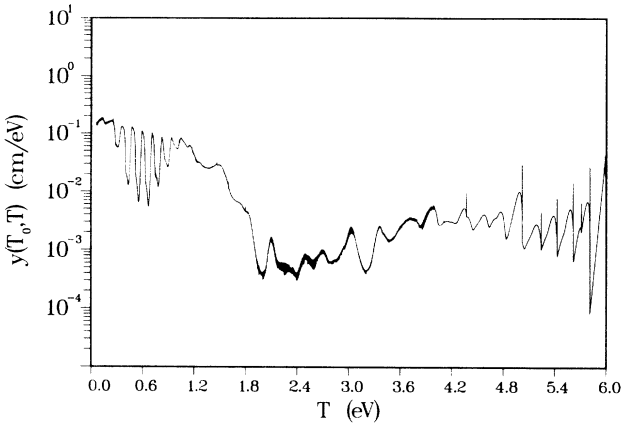

FIG. 4. Electron-degradation spectrum of a 6-eV electron in 75% O_2 and 25% N_2.

process, but only to a minor extent. The real interest lies in the mixtures presented for an initial energy of 6 eV in Figs. 3–6 for changing O_2 concentration. We immediately notice that the characteristic signature of the resonance in vibrational excitation in nitrogen at 2 eV appears even when a concentration of N_2 is only 10% of the total. Another striking feature is the rapid damping of the periodic oscillatory structure of O_2 that arises from the Lewis effect near the source-energy regions as the O_2 concentration decreases. This feature is a direct effect of the increasing competition for electron degradation with strong vibrational excitations of N_2. The characteristic feature that is due to the resonance in N_2 around 1.5–3.5 eV is pronounced in all the figures (at any N_2 concentration).

Until now, very little has been said about the characteristic sharp maxima and minima that are due to resonances in O_2 below 1.3 eV. The effect of these shape resonances is weakened quite rapidly as the concentration of N_2 increases, because of the stronger influence of the resonance in vibrational excitations in N_2 for electrons moderating into this region. This effect greatly reduces the contribution usually attributed to O_2 in this region. However, the importance of the vibrational excitations of O_2 on electron degradation should not be overlooked, because it plays an important role in understanding and predicting yields as will be seen in Sec. III B. Calculations at different incident energies (not shown) support most of the above observations: for incident energies of 3 eV, the strong resonance in N_2 again overwhelms the degradation as the source energies decrease. The results (source energy of 3 eV) show that the addition of a small amount of N_2 both completely erases the trace of a signature of O_2 seen around 2 eV and tremendously reduces the signatures of O_2 resonances below 1 eV. The degradation spectrum in the (75% O_2+25% N_2) mixture is similar to that in the (25% O_2+75% N_2) mixture. Here again, we notice the extreme nitrogenlike characteristics of the degradation spectrum and the rapid decay of the oxygenlike characteristics from the spectrum.

A few words about the CSDA are in order here. The CSDA is transparent in its meaning and is a convenient tool to guide our understanding of degradation. Our previous studies [1,3] have shown that the CSDA is qualitatively and quantitatively reasonable for N_2, but not for O_2. We can expect the CSDA to become increasingly valid as the concentration of N_2 increases above a non-

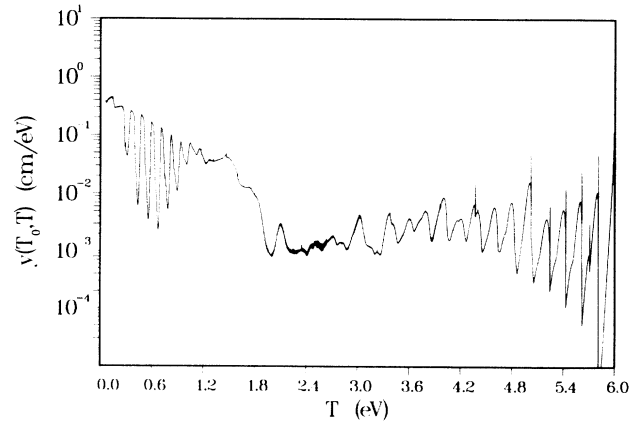

FIG. 3. Electron-degradation spectrum of a 6-eV electron in 90% O_2 and 10% N_2.

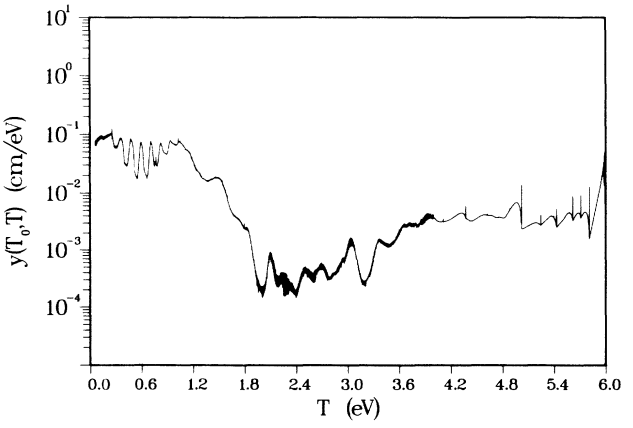

FIG. 5. Electron-degradation spectrum of a 6-eV electron in 50% O_2 and 50% N_2.

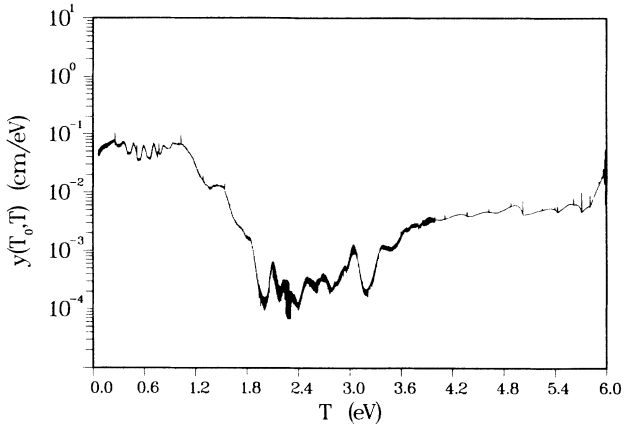

FIG. 6. Electron-degradation spectrum of a 6-eV electron in 25% O_2 and 75% N_2.

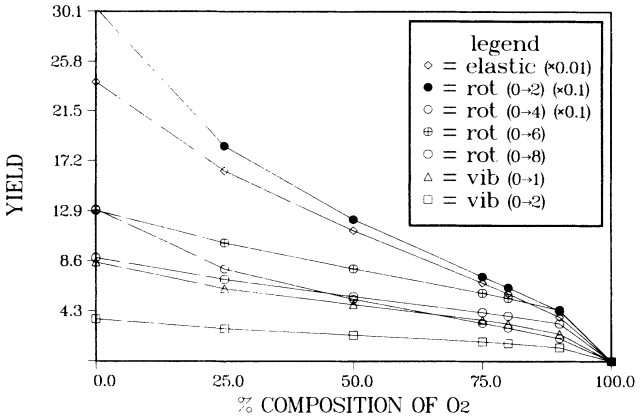

FIG. 8. Yields of products from N_2 as a function of O_2 composition.

trivial amount because of the rapid convergence of the degradation spectrum to a smoother nitrogenlike spectrum. Both because of this finding and the reasonable agreement of the total yield calculated by the CSDA and the SF, we expect the time-dependent CSDA to be a useful tool in studying the time-dependent degradation of electrons.

B. Yields

Table I shows numerical values for the total yields as a function of the composition of O_2, calculated by the SF method. Figures 7 and 8 show the same data in a graphic format for O_2 processes and N_2 processes, respectively. Total yields were calculated by integrating Eq. (5) from the incident energy of 6 eV to the termination energy of 0.06 eV.

Oxygen-nitrogen mixtures are interesting in that the redistribution of yields shows some clear patterns as the concentrations are altered. This is typically demonstrated by O_2 processes when the concentration of N_2 is relatively low. In general, total yield formations fall into three distinctive classes. (i) One pattern is characterized by a high yield of a particular process in a pure gas. The yield falls somewhat as the second gas is introduced and eventually approaches the expected nearly linear decrease. Alternatively, this first pattern may be characterized by a near linearity in concentration. A typical example is the electronic excitation $a\,^1\Delta_g^+$. (ii) The second pattern is characterized by a peak yield in a region other than that in the pure gas and is exemplified by O^- formation. (iii) The third pattern is characterized by a rather sharp change in the yield for a small change in composition or by a high nonlinearity of the concentration. This pattern is seen in rotational excitation.

The first pattern is seen in the relation of the N_2 vibrational excitation with the yields of the electronic excitation to the $a\,^1\Delta_g^+$ and $b\,^1\Sigma_g^+$ states of O_2. The dominance of the N_2 vibrational excitations in the 2–4-eV range, where these channels evolve many of their excitations, explains the linear decay of yields once a nontrivial amount of nitrogen is present. When these vibrational channels are established, very little energy is left for channels that are competing individually for O_2. This fact prevents any major redistribution in or perturbation of the degradation mechanism; i.e., one channel is unlikely to suddenly exert

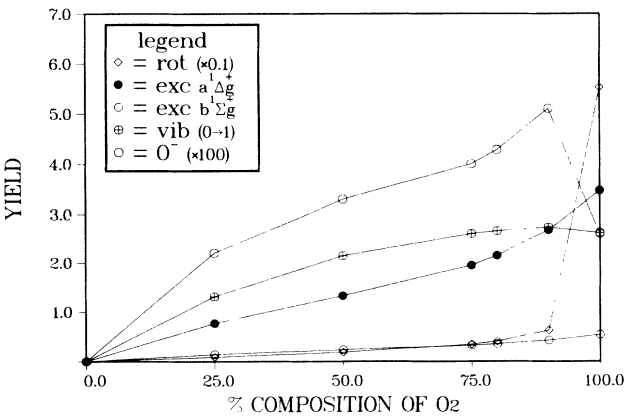

FIG. 7. Yields of products from O_2 as a function of O_2 composition.

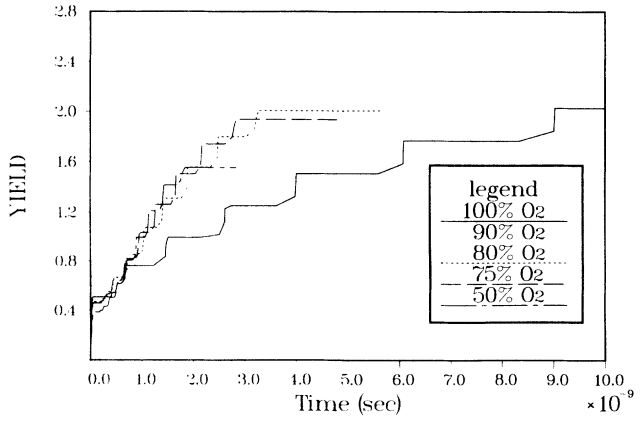

FIG. 9. Time-dependent yields of O_2 vib(0→1) excitation as a function of O_2 composition.

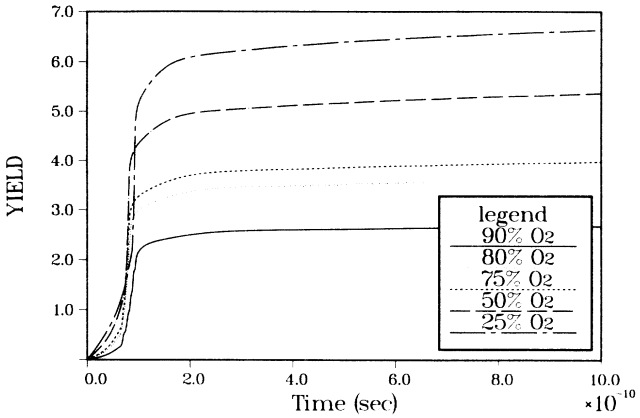

FIG. 10. Time-dependent yields of N_2 vib($0\rightarrow1$) excitation as a function of O_2 composition.

itself, causing thereby, a redistribution of yield. This dominance of the vibrational excitations of N_2 overwhelmingly controls other yields so that changes of concentration have little effect beyond 10% N_2. Hence linear behavior is recovered over a large range of concentrations up to 100% N_2. The behavior of these channels at high O_2 concentrations is a direct consequence of the presence of other large-energy-loss processes. As we introduce the degradation of N_2 channels (which, as noted earlier, tend to establish themselves as major energy-loss mechanisms), less energy is available for the O_2 channels, even for small amounts of N_2. As would be expected, low-threshold excitation channels such as $a\,^1\Delta_g^+$ are more susceptible to this effect. This is illustrated by comparing $a\,^1\Delta_g^+$ to $b\,^1\Sigma_g^+$ excitations at high oxygen concentrations.

The second pattern, composed of O^- formation and, to a lesser extent, vib($0\rightarrow1$) excitation processes, may seem somewhat unnatural at first because the yields for a process increase while the number of species necessary to elicit that excitation process decrease. Yet this pattern has a simple explanation that is based on the competition between two processes. The first process is the introduction by N_2 of numerous energy-loss channels that are out of phase with the vibrational and electronic excitations of O_2. This introduction diverts the energy-loss processes and changes the effectiveness of each distribution. This effect, which manifests itself as a damping of oscillatory structures in the degradation spectra of pure O_2, as in Fig. 1 (see Sec. III A), causes increased yields. The addition of competing processes that help to reduce the yields of other processes in effect pillages the energy available for these processes in O_2. Vib($0\rightarrow1$) excitations behave slightly differently from O^- formation because of their reintroduction at low-energy levels, i.e., the nine sharp resonance peaks. Here the ability of N_2 to compete with these processes offsets some of the gain in excitations at small N_2 concentrations.

The third pattern, rotational excitation, falls at a faster rate than the electronic excitations since rotational excitation suffers from competition in another region, <1.4 eV, as well. In pure O_2, this is a less efficient region in terms of energy loss and is dominated by two low-excitation processes, rotational excitation and momentum transfer, with a few intermittent vibrational excitations accounting for most of the energy loss. With the addition of N_2 and its numerous rotational excitations, in

TABLE I. Relative yields for various processes in O_2 and N_2 as a function of the O_2 composition.

Molecule	Process	(%) Composition of O_2 100	90	75	50	25	0
O_2	Rotational excitation						
	1–3	55.26	6.232	3.454	1.854	0.878	
	Electronic excitations						
	$a\,^1\Delta_g$	3.470	2.675	1.957	1.327	0.768	
	$b\,^1\Sigma_g^+$	0.536	0.422	0.324	0.236	0.143	
	Vibrational excitations						
	$0\rightarrow1$	2.612	2.734	2.597	2.141	1.309	
	$0\rightarrow2$	1.279	0.416	0.335	0.274	0.181	
	$0\rightarrow3$	0.140	0.208	0.167	0.13	0.090	
	$0\rightarrow4$	0.070	0.104	0.084	0.069	0.045	
	O^- formation	0.026	0.051	0.040	0.033	0.022	
N_2	Rotational excitations						
	$0\rightarrow2$		43.13	72.48	121.9	184.6	304.3
	$0\rightarrow4$		19.41	32.44	53.05	79.04	130.6
	$0\rightarrow6$		4.383	5.838	7.925	10.15	12.96
	$0\rightarrow8$		3.215	4.168	5.532	7.011	8.876
	Vibrational excitations						
	$0\rightarrow1$		2.333	3.517	4.848	6.208	8.489
	$0\rightarrow2$		1.166	1.663	2.219	2.767	3.605

this region, appears this weak energy-loss pattern. This increased competition aids the rather dramatic fall in the yields that accompanies small additions of N_2. (However, this conclusion is subject to the qualifications on the cross-section data we used, and is therefore tentative. Swarm experiments generally indicate more efficient energy losses due to oxygen at energies below 1 eV.)

The yield behavior of N_2 (Fig. 8) is far smoother and nearly linear. This feature can generally be explained by the effect of the dominant resonance in vibrational excitations for N_2. However, a few key issues should be pointed out. Again, the center regions at 25–90 % O_2 are highly linear because of the strong dominance exhibited by strong resonances in vibrational excitations of N_2. The sharp drop in yields at O_2 concentrations approaching 100% is the exact opposite of what is due to O_2 processes; i.e., N_2 excitations decrease because O_2 processes are dominant. In the O_2 composition region of 25–90 %, we note a negligible contribution from low-energy excitation processes (such as rotational excitation) that is similar to the pattern in O_2. However, the overall trend of all yields for N_2 is quite similar and shows more linearity than does the trend for O_2. This observation, again, indicates the strong dominance of N_2 in the degradation process.

C. Time-dependent yields

Figures 9 and 10 show time-dependent yields for the $(0\rightarrow 1)$ vibrational excitation of the O_2 and N_2, respectively, as calculated by the time-dependent CSDA. As mentioned in Sec. III A, we expect the CSDA to be a reasonable approximation for the time-dependent case because of the rapid convergence to a nitrogenlike degradation spectrum. However, a more rigorous and detailed study of time-dependent aspects of the subexcitation electron based on the rigorous time-dependent SF theory is planned to be reported in a forthcoming paper [12]. These figures elucidate many of the ideas mentioned earlier in the text.

Electron energies were not plotted in Figs. 9 and 10 because they are a function of composition as well and therefore change for each curve. However, the usual clues presented in Fig. 9 reveal the approximate energy ranges. For example, the sharp, steplike structures that follow the initial burst (within 1.0×10^{-10} sec in Fig. 9) correspond to the nine sharp resonance peaks of the O_2 $(0\rightarrow 1)$ vibrational excitation below 1.3 eV. This observation places the majority of the time-dependent yield spectrum below the 1.4-eV range, with the 6–1.4-eV range occurring in the first 3×10^{-10} sec.

These figures, especially Fig. 9, show the actual phase shifts that occur in yield production, especially below 4.0×10^{-9} sec, as concentrations are altered. Figure 9 also illustrates that optimum concentrations exist for the most efficient energy losses over a particular energy band. This efficiency is not necessarily a linear function of concentration (Fig. 8). In our example of the 50% O_2 mixture, the yield of vib$(0\rightarrow 1)$ excitation becomes saturated first and is most efficient at energy losses that cover a sizable portion of the mid-energy band. A fine steplike structure can be seen, at 90% O_2 concentration, below 3×10^{-10} sec. This structure is a direct consequence of the oscillations induced in the vibrational cross section of N_2 by resonances. The large steplike structures in the yields are quite noticeable, even at 50% O_2 concentration. This is because the dominant contribution to vib$(0\rightarrow 1)$ excitation comes from the resonances below 1.3 eV.

The N_2 yields shown in Fig. 10 have somewhat less dramatic shapes, as expected. However, one important aspect is the early behavior of N_2 vib$(0\rightarrow 1)$ excitation. Although the asymptotic yields curve is nearly linear as a function of O_2 composition, this is not necessarily true at intermediate (early) times. As the O_2 concentration decreases, the N_2 vib$(0\rightarrow 1)$ yield more sharply increases below 0.5×10^{-10} sec. However, the trend of the N_2 vib$(0\rightarrow 1)$ yield reverses, particularly between 25% O_2 and 50% O_2 at $0.5\times10^{-10}<\text{time}\leq 1.0\times10^{-10}$ sec, reflecting the effective roles of certain O_2 concentrations in the early stage of degradation.

IV. CONCLUSIONS

Oxygen-nitrogen mixtures offer some unique insights into the subject of subexcitation electrons, on which very little theoretical work is available. Our major finding is that components do not necessarily contribute equally to electron-degradation mechanisms. The case studied here shows predominance by a single gas, N_2. The rapid convergence to nitrogenlike degradation brought about by the dominance of N_2 is primarily due to resonances in the vibrational-excitation cross sections near 2 eV. To gain further understanding of subexcitation electron behavior, it is important to study temporal aspects of the degradation spectrum. Such a study, based on the time-dependent SF, is now underway [12]. Furthermore, it may be worthwhile to repeat the same calculation, but using the different cross-section data, that was determined by the electron-swarm measurements [9], to examine the electron degradation and its consequences. The study along this line is being planned.

ACKNOWLEDGMENTS

This work was supported in part by the U.S. Department of Energy, Assistant Secretary for Energy Research, Office of Health and Environmental Research, under Contract No. W-31-109-Eng-38. M.A.I. received partial support from the Division of Educational Programs, Argonne National Laboratory.

*Visitor from Department of Electronic Engineering, the University of Minnesota.

†Also at Department of Physics, Rice University, Houston, TX 77251.

[1] K. Kowari, M. Kimura, and M. Inokuti, J. Chem. Phys. **89**, 7229 (1988).

[2] A. Pagnamenta, M. Kimura, M. Inokuti, and K. Kowari, J. Chem. Phys. **87**, 6220 (1988).

[3] M. A. Ishii, M. Kimura, M. Inokuti, and K. Kowari, J. Chem. Phys. **90**, 3081 (1989).
[4] M. A. Ishii, M. Kimura, and M. Inokuti, Phys. Rev. A **42**, 6486 (1990).
[5] K. Kowari, M. Inokuti, and M. Kimura, Phys. Rev. A **42**, 795 (1990).
[6] M. Inokuti, M. Kimura, and M. A. Dillon, Phys. Rev. A **38**, 1217 (1988).
[7] Y. Itikawa, M. Hayashi, A. Ichimura, K. Oda, K. Sakimoto, K. Takayanagi, M. Nakamura, N. Nishimura, and T. Takayanagi, J. Phys. Chem. Ref. Data **15**, 985 (1986).
[8] Y. Itikawa, A. Ichimura, K. Onda, K. Sakimoto, K. Takayanagi, Y. Hatano, M. Hayashi, H. Nishimura, and S. Tsurubuchi, J. Phys. Chem. Ref. Data **18**, 23 (1989).
[9] G. Gousset, C. M. Ferreira, M. Pinheiro, P. A. Sá, M. Touzeau, M. Vialle, and J. Loureiro, J. Phys. D **24**, 290 (1991).
[10] H. S. W. Massey and E. H. S. Burhop, *Electronic and Ionic Impact Phenomena* (Oxford University Press, London, 1952), Table VI, p. 279.
[11] S. A. Lawton and A. V. Phelps, J. Chem. Phys. **69**, 1055 (1978).
[12] M. Kimura, T. Teng, and M. Inokuti (unpublished).